Fracture Mechanics of Concrete,
edited by F.H. Wittmann, 1983
Elsevier Science Publishers B.V., Amsterdam — Printed in The Netherlands

Chapter 2

STRUCTURE OF CONCRETE WITH RESPECT TO CRACK FORMATION

by F.H. WITTMANN

1. INTRODUCTION

There are many papers on specific details of the structure of hardened cement paste and concrete. The wide range of literature begins with microscopical observation and purely phenomenological description and follows through to real mathematical models. In this contribution, we will try to summarize and discuss only those structural aspects which are directly linked with crack formation and failure processes. A more general treatment of modelling the structure and performance of concrete has been published recently (ref. 1).

Until now many structural details of the porous and composite materials were not known well enough. Therefore the existing knowledge has been condensed into several models. This is one possibility to describe the real behaviour in a simplified and approximative way. As new information is available these models can be adjusted continuously.

It has been proven to be advantageous to subdivide the structure of concrete into different levels. In Table I a hierarchic system of three different levels is shown. This means that the models on the different levels are interrelated in a systematic way, or more precisely models on a given level are based on the results of the previous level.

At the micro-level the structure of hardened cement paste is treated. So far, the only model which gives us quantitative results on the micro-level is the Munich Model (ref. 2). Therefore we will choose this model among the different existing materials science models as the basis for further discussion.

The observed behaviour of concrete cannot be linked directly with microstructural mechanisms because there are additional factors within the hierarchic structural system which interfere. In concrete the most important factors are pores, cracks, and inclusions. These structural details of a composite material will be introduced on the meso-level.

The final aim of the hierarchic structural system is, of course, to characterize the macroscopically observed behaviour of a given material in a realistic and rather general way. On the macro-level the information which results from the two previous levels will be used to describe the materials behaviour in

TABLE I

Characteristic structural features of hardened cement paste and concrete subdivided into three different levels and corresponding types of models.

Structural Level	Characteristic Features	Type of Models
Micro-Level	Structure of Hardened Cement Paste, Xerogel	Materials Science Models
Meso-Level	Pores, Cracks, Inclusions, Interfaces	Materials Engineering Models, Mechanical and Numerical Models
Macro-Level	Geometry of Structural Elements	Structural Engineering Models, Material Laws

such a way that it can be used directly in structural engineering and design. In this context macroscopic fracture mechanics parameters have to be considered.

In the following sections the three different structural levels will be dealt with consecutively. The interrelationship of results obtained at different structural levels will be outlined in particular.

2. MICRO-LEVEL : HARDENED CEMENT PASTE

2.1 Introductory rermarks

In concrete, a heterogeneous multi-phase material, different kinds of aggregates may be cemented by hydraulic cement paste to form an artificial stone. The properties of the resulting material depend both on the type of aggregate and the hardening matrix. Most typical aggregates may be assumed to react in reasonable approximation as linearly elastic. Hardened cement paste, however, is known to be a viscoelastic material. Depending on the relative humidity of the surrounding atmosphere the microporous structure of hardened cement paste contains a considerable amount of adsorbed and capillary condensed water. As the water content is changed shrinkage or swelling occurs. The hygral length change of concrete, however, is restrained by the inert aggregates. As a consequence a complex state of internal stresses is built up. The coefficient of thermal dilatation of aggregate and hardened cement paste may vary by a factor of up to 5. It is well known that the elastic moduli also differ to a great extent in most concretes. Therefore a complex state of internal stresses is also created when the temperature is changed or an external load is applied.

Most aggregates used in concrete technology, being approximately linearly elastic within the range of service loads, show no drastic influence of relative humidity of the surrounding air or of temperature on the elastic modulus, on strength and on the coefficient of thermal expansion. The properties of those materials can be realistically described with the help of simple and idealized expressions.

The highly dispersed hydration products of portland cement react to changes of the environment in a far more complicated way. Nearly all characteristic properties of hardened cement paste can be directly linked with the mutual interaction of colloidal particles and/or with the interaction of the total gel structure with water. The presence of aggregates in concrete moderates the actual behaviour of pure hardened cement paste. Therefore on the micro-level we will discuss the structure of hardened cement paste and the interaction of the xerogel with water.

Among the essential reasons why concrete has become the most extensively used building material of our day is the fact that it is comparatively cheap and also that even unskilled personnel under certain conditions may produce concrete with satisfactory serviceability. This situation is not really a challenge for research in this field. As a consequence it is not surprising that so far, very little on the physical basis of the materials properties is really known.

Concrete structures, however, have become increasingly more sophisticated. Cementitious materials are now used under extreme conditions : high temperatures, low temperatures, impact loading conditions, etc. It is essential for a simultaneously economic and safe application of any material that its behaviour while under service can be accurately predicted. This aim, however, can only be achieved via a better understanding of the structure of hardened cement paste and its relation to the macroscopically observed behaviour. As mentioned above this problem will be approached by introducing three different hierarchic levels of structure.

Some investigators tried to develop models of the microstructure of hardened cement paste on the basis of comparatively crude mechanical tests on concrete. These early models had a purely phenomenological character and they can only be used to describe the observed behaviour under given conditions. As fundamental research on the microstructure proceeded, new and more realistic models were created. With the help of these models the actual complex situation within a gel were to be described in a simplified manner. Even these models should not be taken too literally but they should rather be judged by the contribution

they provide for a more comprehensive understanding of the total system.

Models will have to be abandoned completely as soon as we have sufficiently detailed and reliable data. So far, however, we definitely need appropriate models. This is the only possibility to accumulate most of the information available. In this way, finally the gap between the research on the microstructure and the engineering properties will be bridged. New results necessarily have to be incorporated in suitable models.

Research on the structure of hardened cement paste can be subdivided into two groups. In one group, mainly a chemical and mineralogical approach is used. In this way the hydration process, the composition, and the crystal structure of hydration products have been studied. An excellent summary of the results obtained in this way has been published by J.F. Young (ref. 3). On the other hand there is a more physics-orientated approach. In the latter mentioned connection the mutual coupling of gel particles and the interaction of gel particles with absorbed vapours are of prime interest. Of course, there is no strict borderline separating these two areas of research.

In this contribution emphasis is placed upon the physical approach because it seems easier to link physical models of the xerogel with crack formation and failure, but some chemical and mineralogical aspects of the structure will be treated first.

2.2 Chemical and mineralogical aspects of the structure

The main compounds in Portland cement are calcium silicates, i.e. $3CaO \cdot SiO_2$ and $2CaO \cdot SiO_2$. The aluminate and ferrite phases are of minor importance with respect to the structure and the mechanical properties of the resulting cementitious material. The hydration of the calcium silicates may be described in a simplified way by the following equations :

$$2(3CaO \cdot SiO_2) + 6H_2O \rightarrow 3CaO \cdot 2SiO_2 \cdot 3H_2O + 3Ca(OH)_2$$
$$2(2CaO \cdot SiO_2) + 4H_2O \rightarrow 3CaO \cdot 2SiO_2 \cdot 3H_2O + Ca(OH)_2$$

These simple expressions, however, are somewhat misleading because the hydration process and the exact determination of the hydration products becomes extremely complex if one goes into detail. Probably the first comprehensive treatise of the chemistry of hydration is provided by the proceedings of the Washington Symposium (ref. 4). In the meantime, a number of additional results on the hydration products have been gathered. Most essential findings have been presented in subsequent meetings in Tokyo (ref. 5), Moscow (ref. 6) and Paris

(ref. 7).

It is quite obvious that progress in this field is comparatively slow. This may be explained by the fact that there are few techniques which may be successfully applied to study the structure of hydration products of cements. Only limited information can be deduced from X-ray diffraction. The same applies to the application of electron microscopy. Much effort has been spent to develop appropriate chemical methods. An early break-through has been achieved by sorption methods (ref. 8). As there are no prevailing methods so far, the actual state of knowledge has to be discussed by combining the relevant information of different approaches.

From the early micrographs (ref. 9 and 10) taken from hydrated cement and hydrated clinker components it became clear that a variety of different particles are to be found. Needles, crumbled or rolled foils and tubes have been observed in hardened cement pastes. The variability of layered silicate hydrates is known from natural minerals. If the silicate tetraeders match the $\{Me(O,OH)_6\}$ -octaeders completely plane sheets are formed. This principle of geometrical fitting has been discussed among others by Liebau (ref. 11). If the just mentioned subunits do not fit completely structures like corrugated iron (crumbled) sheets or rolled foils are formed. In the case of calcium silicate hydrates, aluminium and ferric ions among other ions may substitute for both silicon and calcium. In addition sulfur may substitute for silicon. The morphology of the gel particles changes as calcium or silicon are substituted (ref. 12). Richartz and Locher (ref. 13) prepared on this basis a vivid graphic model of different morphologies in hardened pastes.

Kantro, Brunauer and Weise (ref. 14) distinguish three stages of the hydration of cement. According to these authors, immediately after mixing with water a skin adhering to the particles of the anhydrous compounds is formed. This first product has a high C/S ratio. In the second stage splitting-off of particles of the skin is observed. The second product formed in this way has a C/S ratio of 1.0 to 1.5. In the electron microscope one detects foils or platelets at this stage. Finally these particles grow to a thickness of about three layers with a C/S ratio of 1.5 to 2.0. Although modified by several authors this concept basically proved to be correct (ref. 15, 16 and 17).

Depending on the C/S mole ratio calcium silicate hydrates may be subdivided into two groups. In aqueous suspensions at room temperature C-S-H (I) with a C/S ratio of 0.8 to 1.5 is formed. The semi-crystalline calcium silicate hydrate with a C/S ratio of 1.5 or above generally is termed C-S-H (II). In hydrated cement paste semi-crystalline and near amorphous products are found. X-ray

powder patterns usually show only three broadened lines. Sometimes this phase was called tobermorite gel. This name was chosen because it was concluded that the hydration products of cement were degenerate varieties of tobermorite. This statement has often been questioned and in fact there is some evidence that some products are degenerate structures of jennite. Therefore it seems reasonable to follow a suggestion made by Taylor (ref. 18) and to use a more general expression i.e. calcium silicate hydrate or in abbreviated form C-S-H. This general term also takes into consideration the fact that there is not a finite number of phases (each of a definite composition and structure) but instead a large continuous range.

Essentially based on sorption experiments, Powers and Brownyard (ref. 8) determined an average particle radius of 140 Å. In this calculation it was assumed that the microstructure is composed of equal spheres. Later Powers (ref. 19) calculated a mean value of $6.6 \cdot 10^6$ Å^3. This value leads to a revised radius of 117 Å. There is no doubt that these values should not be taken too literally but they are a strong indication that hydration products are of colloidal dimensions.

More recently Grudemo (ref. 20) suggested a different structure of the hydration products. The fact that basal reflexions are not observed in the region of 9 - 15 Å may indicate that layered or lamellar structures are rare. Therefore Grudemo concludes that cement gel is a submicrocrystalline mixture of structural elements. Some of them are related to tobermorite and some are related to jennite whereas others are related to CH-portlandite. In this concept, gel pores are formed as silica chains and are left out during the growth of the structure. If this assumption holds true pores with a diameter of 9 Å or multiples thereof must be expected.

If the pore size distribution is determined from sorption data a maximum at a radius of about 18 Å is found (ref. 21 and 22). At much lower radii this method to determine pore size distributions looses its significance. It may be mentioned, however, that often a second maximum is recorded at about 8 to 10 Å. This fact would confirm the Grudemo's concept. The observed pore size distribution, however, depends on the preparation of the hydrate sample. Therefore it might be tempting to compare experimentally determined pore size distribution with results of morphology studies of C-S-H.

Another promising approach to the microstructure of hydration products has been put forward by Tamas (ref. 23). Tamas studied polymerization of $Si\,O_4^{4-}$ monomers. In the meantime, this interesting approach to study the microstructure has been considerably extended (see f.e. ref. 24). Rio and his co-workers (ref. 25) also studied the hydration process on a macromolecular level. They tried to

correlate the mechanical behaviour and the morphology with the degree of condensation of the silicate hydrates.

Based on sorption data the internal surface of fully hydrated cement paste is found to be 100 - 200 cm^2/g. Considerably higher values have been calculated by Winslow (ref. 26) who used small angle X-ray scattering. His findings are discussed in detail with respect to the structure and properties of hardened cement paste by Copeland and Verbeck (ref. 27).

The actual state of knowledge on the structure and composition of hydrates has been reviewed by Taylor and Roy (ref. 28). Structure formation and development in hardened cement pastes have been discussed by Sereda and co-workers (ref. 29). The major components of the microstructure of a xerogel, i.e. solid phase, pores, and water, have been treated separately and discussed in connection with properties of hardened cement paste by Wittmann (ref. 30).

This compilation of information on the microstructure of hardened cement paste is, by no means, complete and it may even seem to be arbitrarily selected in some respect. For the present purpose we may conclude, however, that although there is a wide field of active research, there are not enough well established data available to understand the microstructure in full detail. Lack of knowledge is the main reason why we have to introduce simplifying models on the micro-level. In the following sections therefore we have to deal with the development of appropriate models.

2.3 Earlier models

Models described in the literature can be subdivided into two groups : Inductive models and deductive models. By taking into consideration all relevant information on the structure such as pore size distribution, mutual interaction of colloidal particles in a xerogel and the characteristic properties of adsorbed water films an inductive model can be developed. The validity of such a model must be checked by a critical comparison of the predictions of the model with the actually observed behaviour of the system. On the other hand one may deduce a model of the microstructure from the experimentally determined macroscopic data. Models of this type have to be tested by comparing them with results of more fundamental work on the structure. Some deductive models are suggested with the aim of covering just one specific point such as influence of moisture content on strength.

A typical example for a deductive model has been given by Ishai (ref. 31). The mechanical behaviour under load has been analyzed and on the basis of the comprehensive results obtained in this way a structural model of hardened ce-

ment paste has been established. There is no doubt that the most detailed information on the structure of hardened cement paste has been gained by sorption methods. The mean particle size and the pore size distribution have been estimated by Powers (ref. 19) as indicated above. Powers summarized his findings in a geometrical model and a physical model (ref. 32 and 33). With the help of the geometrical model the pores of the structure are subdivided into gel pores and capillary pores. The physical model of Powers serves as a basis for a thermodynamic treatment of partially water filled micro pores. Within the framework of this inductive model, Powers deals with three basic mechanisms :

a) Change of surface tension of the colloidal particles.

b) Change of disjoining pressure in narrow gaps.

c) Change of hydrostatic tension.

The most important feature of this model probably is the load bearing capacity of water adsorbed in zones of hindered adsorption.

Within the thermodynamic models it is presumed that colloidal particles do not change their structure and/or composition significantly as the moisture content of the system changes. Bernal (ref. 34) has demonstrated, however, that the structure of C-S-H (I) changes during drying. The c-spacing of a unit cell goes down from 14 to 9 Å. It may be concluded that during severe drying, this material loses interlayer water. On this basis Feldman and Sereda proposed another model for hydrated portland cement (ref. 35-37). With the help of this model it is tried to link shrinkage, creep and the influence of moisture content on the elastic modulus with the exchange of interlayer water.

All models described above have been modified by various authors. In some cases major components of a model have been adapted and used for the interpretation of experimental findings. Hope and Brown (ref. 38), for instance, used Feldman and Sereda's model to postulate a possible mechanism of creep.

For many years there has been a lively controversy on the validity of different models. So far, no generally accepted agreement could be reached. But it seems that by now most people concerned have realized that different models may contribute to progress in various ways and that one single model is not able to characterize the complex situation.

Kondo and Daimon (ref. 39) have developed another inductive pore model for C-S-H gel. In this essentially geometrical model clusters of crystallites are separated by inter gel particle pores. In each gel particle there are inter-crystallite pores and finally intra-crystallite pores are found in individual crystallites. This model may partially bridge the gap between the two opposing models of Powers-Brunauer and Feldman-Sereda if it is realistic to compare the

inter-crystallite pores with traditional micro pores and the intra-crystallite pores with interlayer space. But the more important question about the extent to which water in micro pores and in interlayer space influences the mechanical behaviour and in particular crack formation and strength still remains untouched.

2.4 The Munich Model

2.4.1 New data forming the basis of the model. With respect to the xerogel of C-S-H the methods used so far may be subdivided into two groups :

a) Direct observations of characteristic properties of the gel.
b) Investigations into the properties of water adsorbed in the colloidal system.

Within the first group the determination of van der Waals forces at low distances, of the surface energy, and of the coupling of individual particles in the gel are of primary interest. The study of the mobility and of the disjoining pressure of adsorbed films in micro-pores plays a dominant role in the second group mentioned above. In the following paragraphs some recent results are briefly summarized.

Classical van der Waals experiments have been restricted to the observation of the interaction at comparatively large distances ($d > 1000$ Å). The properties of a xerogel, however, are only affected by attractive forces acting between solid surfaces which are separated by micro-pores. That means, they are separated by distances of a few Ångströms. If these micro-pores will be separated by a crack, van der Waals forces contribute to the energy consumed.

The theoretical background as well as experimental techniques had to be extended so that the range of short distances could be investigated (ref. 40). By evaluating the bending line of a thin quarz plate which was mounted on a solid quarz support at a certain distance it was possible to determine the van der Waals attractive force down to about 80 Å (ref. 41). With the help of theoretical considerations it is possible to extrapolate beyond the range of experimental data with a reasonable degree of reliability to colloidal distances.

The van der Waals attraction is strongly dependent on the dielectric properties of the medium which is between the interacting surfaces. As a consequence the van der Waals attraction is diminished as water is adsorbed on two opposing surfaces. The influence of adsorbed films on van der Waals forces has been studied carefully as a function of film thickness (ref. 41). Adsorbed water reduces the attractive force approximately by one order of magnitude.

There is a close correlation between van der Waals attraction and surface

free energy (see e.g. ref. 42). Therefore the dependence of surface free energy on the thickness of adsorbed water films may be directly deduced from the observed decrease of van der Waals attractive force. By comparison of results obtained by independent methods this is shown in references (41) and (43). In a more direct way the change of surface free energy can be calculated with the help of a thermodynamic approach from sorption data (ref. 22). Starting from the dry state the surface energy decreases sharply as the water vapour pressure is increased. Above $p/p_0 = 0.5$ the resulting change, however, is comparatively small. We will compare this result directly with the influence of moisture content on strength.

Primary bonds and secondary bonds both contribute to the mutual coupling of gel particles within a xerogel. The mechanical properties of the system of course depend primarily on these coupling forces. It could be shown that Mössbauer's spectroscopy is a powerful tool to investigate the coupling of gel particles (ref. 44). If the water vapour pressure is raised above a certain level, the disjoining pressure of water separates surfaces which are exclusively held together by van der Waals bonds. The disjoining pressure may be subdivided into different components each having a different physical origin (ref. 45). By extending the van der Waals experiments mentioned above to the range of high vapour pressures the action of disjoining pressure could be observed directly (ref. 46). Stockhausen has later discussed the disjoining pressure and its meaning for C-S-H (ref. 47).

The mobility of adsorbed water is a decisive factor in a number of models. If the first adsorbed layers had an ice-like structure the creep mechanism could be traced back to displacements within this modification. Using the Debye theory the viscosity of liquids can be deduced from dielectric measurements. Schlude and Wittmann determined the complex permittivity in the range of microwave frequencies (ref. 48), and Zech and Wittmann in the range of Hertzian spectroscopy (ref. 49). By comparing these results with NMR measurements one can conclude that the viscosity increases with decreasing thickness of the adsorbed layer. In the region of a monolayer, however, the definition of viscosity looses its significance. In this case a high mobility of water molecules along the surface is observed but the molecules are hindered from leaving the surface. Under these conditions, the adsorbed films are called a two-dimensional van der Waals gas.

In the next section some general relations will be introduced. With the help of these relations it is possible to describe the xerogel of hydrated portland cement

realistically. In this context,of course,drastic simplifications are still inevitable.

2.4.2 Elements of the model. It is well known that a liquid droplet having a radius r is under a hydrostatic pressure P :

$$P = \frac{2\gamma}{r} \tag{1}$$

In equation (1) γ represents the surface tension of the liquid. In a liquid, surface tension and surface energy are numerically equal. In solids these two values are at least in the same order of magnitude. In a colloidal system non-spherical particles can exist. Flood (ref. 50) has shown that the mean pressure in solid particles created by surface tension in such a system can be estimated with the help of the following equation :

$$P = 2\gamma \frac{S}{3} \tag{2}$$

S stands for the specific surface area and has to be expressed as cm^2/cm^3 in this connection. If the specific surface area is introduced instead of the radius the actual particle size distribution is neglected or rather replaced by a mean value. In C-S-H there are particles which are large enough to ensure that no appreciable internal pressure will be created by surface tension. Other particles in the same system will experience comparatively high pressures. The overall response of a system with active and inactive particles has been calculated by Krasilnikov and co-workers (ref. 51). In their paper it is pointed out that expansion of gel particles in a heterogeneous system is not linearely related to the expansion of the total system but a geometrical magnification factor has to be taken into consideration.

Well aware of the implied simplifications we may go back to equation (1). Now r has to be looked at as a characteristic value of a given xerogel and P as a mean internal pressure. The resulting internal pressure changes as the surface energy is changed. The surface energy or rather the interfacial energy of a colloidal system may be changed by adsorption of gases or vapours. If a film of thickness Γ is adsorbed at a given vapour pressure P the interfacial energy measured in vacuum decreases by $\Delta\gamma$ (ref. 52) :

$$\Delta\gamma = \gamma_0 - \gamma = RT \int_0^p \Gamma \, d(\ln p) \tag{3}$$

If γ of equation (3) is inserted into equation (1) the change of internal pressure caused by a changing surface energy can be calculated. Each individual gel particle expands as the internal pressure is reduced. Bangham and co-workers showed that within certain limits, a linear relation exists between the change of interfacial energy and the resulting length change (ref. 53) :

$$\frac{\Delta l}{l} = \lambda \, \Delta\gamma \tag{4}$$

Later Hiller expressed λ in terms of properties of the colloidal system (ref. 54). It is assumed that in the range of low RH the hygral length change can be described semi-phenomenologically by utilizing equation (4). A more quantitative application of equation (4) is not possible as decisive factors such as the particle size distribution are not sufficiently well known.

As the relative humidity is raised above 50% some surfaces will be separated by disjoining pressure (ref. 46). This leads to additional expansion of the colloidal system. This length change is not caused by a corresponding change of surface energy. Therefore equation (4) cannot be applied in this range. Simultaneously the total structure is weakened by the action of the disjoining pressure.

The Griffith-criterion has proved to be very successful in describing fracture phenomena in hardened cement paste and concrete (ref. 55). According to this concept the square of the related strength is equal to the related interfacial energy :

$$\left(\frac{\sigma}{\sigma_0}\right)^2 = \frac{\gamma}{\gamma_0} = 1 - \frac{\Delta\gamma}{\gamma_0} \tag{5}$$

By inserting equation (3) into equation (5) the relative strength decrease as a function of moisture content can be estimated (ref. 56). By using Bangham's equation (4), equation (5) may be rewritten :

$$\left(\frac{\sigma}{\sigma_0}\right)^2 = 1 - \frac{1}{\lambda\gamma_0} \cdot \frac{\Delta l}{l} \tag{6}$$

Equations (5) and (6) indicate a linear relationship between the square of the related strength and change of interfacial energy and length change respectively. This statement, of course, is only valid in the range of RH in which drying or rewetting changes the interfacial energy only. As mentioned above at high moisture content the action of disjoining pressure cannot be neglected and therefore additional weakening of the structure has to be anticipated.

In conclusion we can say that the Munich Model introduces two terms which can be related to strength and failure of concrete :

a) Interfacial energy of the xerogel.

b) Disjoining pressure of adsorbed water films.

2.4.3 Comparison with experimental results. Theoretical predictions of the Munich Model are compared with experimental results in references (2) and (57). There the influence of moisture content on hygral length change (swelling and shrinkage), on modulus of elasticity, on damping, and on creep, is discussed. Here we will concentrate on strength exclusively.

Wittmann has measured strength of hardened cement paste as function of moisture content (ref. 56). In this paper (ref. 56) it has been shown that the square of the related strength decreases linearely with increasing swelling. This relation is predicted by equation (6). Above 50% RH, however, there is additional length change observed due to the action of disjoining pressure.

If we replot experimental data of reference (56) as function of change of interfacial energy we find the relation plotted in Figure 1. For two different values of water/cement ratio, a straight line is obtained in the low humidity region. Above 50% RH the disjoining pressure further weakens the microstructure and hence causes a further decrease of the related strength.

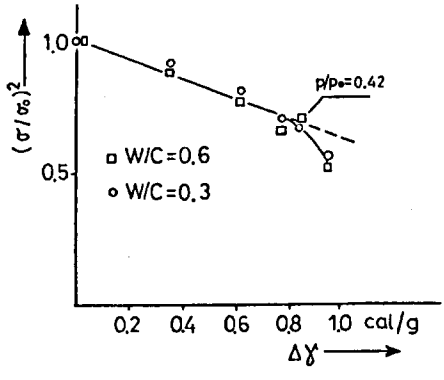

Fig. 1. Square of the related compressive strength of hardened cement paste cylinders as function of change of interfacial energy. Results of two test series (ref. 56) with differing water/cement ratio are shown.

Comparable test series have been carried out under carefully controlled conditions by Pihlajavaara (ref. 58). Experimentally determined values of flexural

strength of mortar prisms have been replotted in Figure 2. Within the range of accuracy again a straight line is obtained in the low humidity range and additional weakening is caused by disjoining pressure at humidities above 50%.

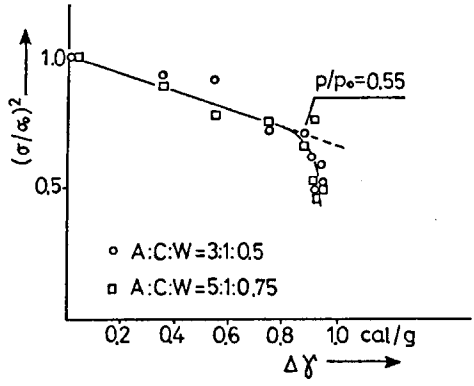

Fig. 2. Square of the related flexural strength of mortar prisms as measured by Pihlajavaara (ref. 58) replotted as function of change of interfacial energy.

The linear relation between the square of the related strength and the change in interfacial energy as documented in Figures 1 and 2 has been predicted by equation (5), a basic relation of the Munich Model.

2.5 Porosity

It has often been tried to relate strength of a porous material directly to the total porosity. In the literature therefore a number of different equations relating strength and porosity can be found. All of them predict an increase of strength as the total porosity decreases. We will not deal with these empirical equations here. By applying these formulae tacitly one assumes that the pore size distribution either is independent of porosity or changes in an analogous way.

This assumption is not fulfilled in many porous building materials. In Figure 3, the pore size distributions of two natural sandstones are shown. In addition the corresponding strengths are indicated in Figure 3. If we based the prediction on the total porosity of the samples only, we had concluded that sample A must have the higher strength. In fact the contrary is observed. The reason for this is that the pore size distribution functions are different. Sample A has more coarse pores than sample B. It is obvious that we have to take into considera-

tion both total porosity and pore size distribution in deriving strength of a porous material.

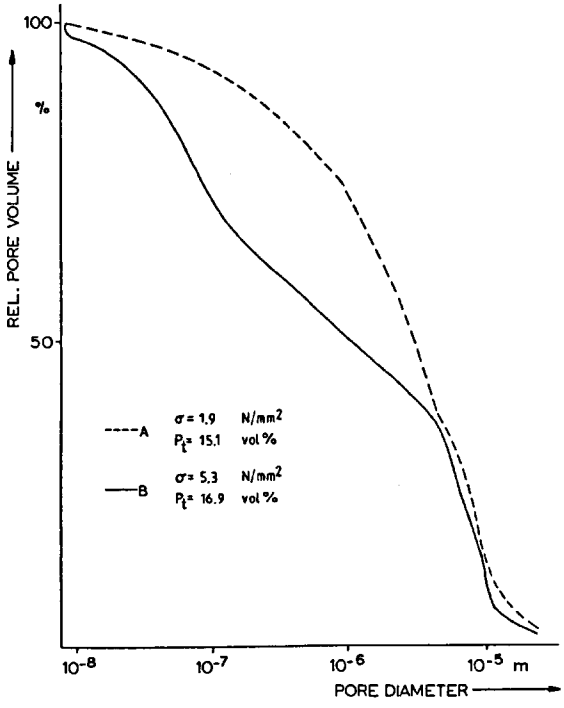

Fig. 3. Pore size distribution of two different types A and B of porous natural stone (sand stone). In addition the total porosity P_t and the biaxial flexural strength R_b of the two materials are indicated.

In concrete technology the water/cement ratio plays a dominant role. In Figure 4 strength of hardened cement paste is shown as function of the water/cement ratio. In addition in Figure 4 the elastic modulus is shown as a function of water/cement ratio.

In Figures 5 and 6 the pore size distribution of hardened cement paste are given as a function of water/cement ratio and as a function of duration of hydration respectively.

Even though the Griffith criterion is a simplified description of the actual failure process we can still use it to discuss the influence of porosity and pore size distribution on strength of hardened cement paste. If we use as usual, σ for strength, E for elastic modulus, γ for the fracture surface energy and 2c

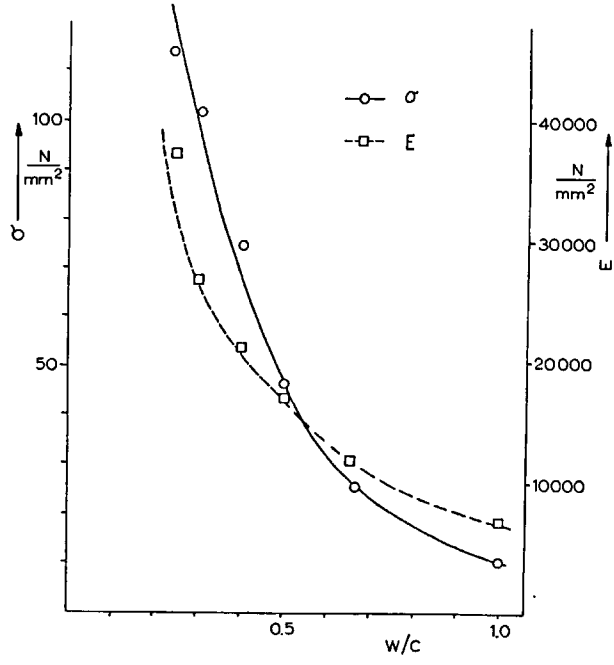

Fig. 4. Influence of water/cement ratio on strength and modulus of elasticity of hardened cement paste.

for the crack length, the Griffith equation reads as follows :

$$\sigma = \sqrt{\frac{2E\gamma}{\pi c}} \tag{7}$$

From Figure 4 we know the influence of water/cement ratio on the elastic modulus E. In fact it can be shown that the elastic modulus depends essentially on the total porosity P :

$$E = E'(P) \tag{8}$$

In fact, the influence of porosity can be adequately predicted by models of composite materials. The fracture surface energy γ is well defined for a non-porous material. If a crack spreads across a porous structure the energy which is consumed depends on the fracture surface energy of the non-porous material and the number N of particles to be cracked per unit area. In other words, this means that only the part of the fracture surface which goes across solid par-

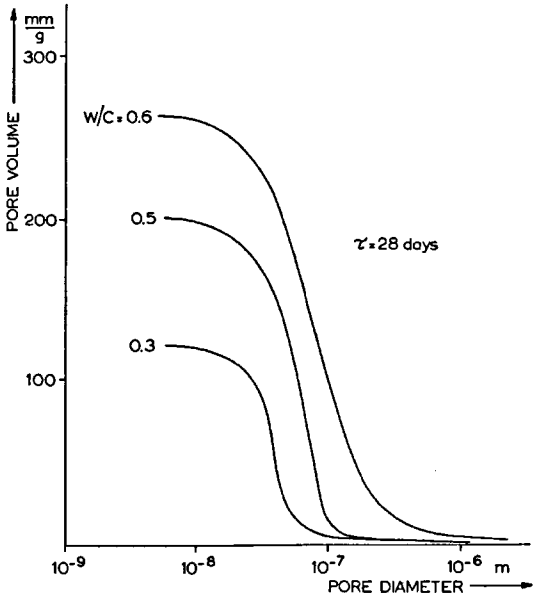

Fig. 5. Pore size distribution of hardened cement paste after 28 days of hydration for three different water/cement ratios.

ticles contributesto the energy balance. This is shown schematically in Figure 7. It is obvious that the effective surface energy depends essentially on the total porosity. In material (A) in Figure 7 the crack passes approximately through 55% of solid matter in its way whereas in material (B) only about 25% of the crack length has passed solid particles. In fact this relation holds true even if one considers a turtuous crack path as has been suggested by Higgins and Bailey (ref. 59).

Then we can redefine the fracture surface energy of a porous material in the following way :

$$\gamma_p = \gamma N = \gamma (1-P) \qquad (9)$$

The fracture mechanism in a xerogel such as hardened cement paste as suggested by Higgins and Bailey (ref. 59), is schematically shown in Figure 8. The meaning of crack length 2c in equation (7) will be further discussed in the following section on structural features of the meso-level.

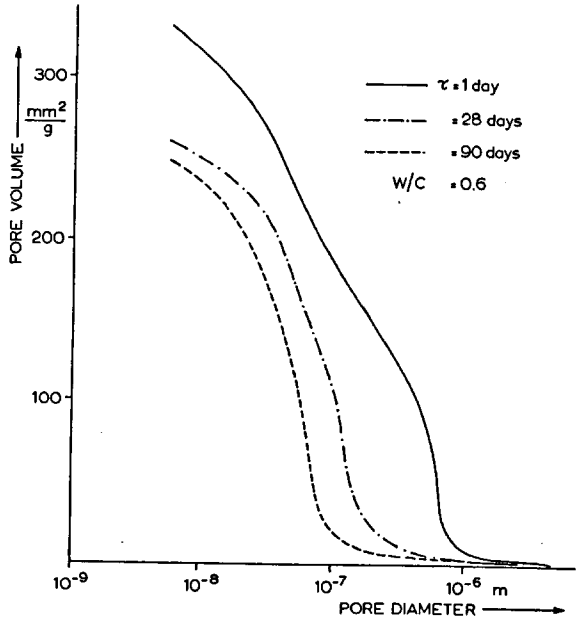

Fig. 6. Pore size distribution of hardened cement paste having a water/cement ratio of 0.6 after 1, 28, and 90 days of hydration.

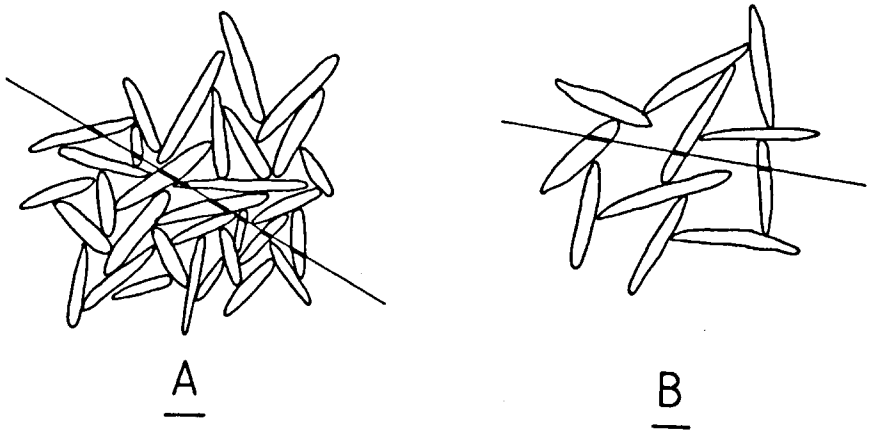

Fig. 7. Schematic representation of fracture energy consumed by a crack running through a material (A) with low porosity and a material (B) with high porosity.

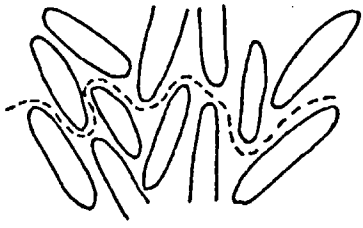

Fig. 8. Fracture mechanism in a xerogel such as hardened cement paste according to Higgins and Bailey (ref. 59).

3. MESO-LEVEL

3.1 General remarks

In the preceeding chapter we have described the microstructure of hardened cement paste and in particular the interaction of the xerogel with adsorbed water. It has been shown that it is possible to predict qualitatively the influence of moisture content on strength of hardened cement paste on this basis.

So far we have neglected, however, the heterogeneous structure of the material. Therefore we will introduce big pores, pre-existing cracks, and inclusions as the main characteristic features of the meso-level.

3.2 Big pores

In Figure 5 the pore size distributions of hardened cement paste with different water/cement ratios are shown. Hardened cement paste prepared under normal conditions always has some big pores which are not covered by the distribution functions shown in Figure 5. These big pores, however, considerably reduce the strength of the material. Recently it has been tried to limit big pores to a minimum, thus increasing the strength.

The crack length 2c in the idealized Griffith criterion (see equation 7) is defined to be the length of one single crack in an otherwise homogeneous infinite plate. In a real porous material it stands for an effective maximum crack length $\bar{C}$ or an equivalent big pore. This value $\bar{C}$ must not necessarily be identical with the existing maximum crack length because there is interaction between large neighboring cracks. In any case it means that C depends sensitively on the pore size distribution (PSD) and in particular on the probability of finding large pores.

$$C = \bar{C}\ (PSD) \qquad (10)$$

Then we can rewrite equation (7) by using equations (8) to (10) in the following way :

$$\sigma = \sqrt{\frac{2 \cdot E'(P) \cdot \gamma(1-P)}{\pi \bar{C}\ (PSD)}} \qquad (11)$$

In doing so we can link structural details of hardened cement paste directly with strength. In many cases $\bar{C}$ has to be determined from fracture tests. Possibly in the future we will be able to estimate the effective maximum crack length $\bar{C}$ by fitting the pore size distribution to an extreme value distribution function.

3.3 Cracks

It is well known that under usual climatic conditions in hardened cement paste, mortar, and concrete, numerous cracks exist before a load is applied. There are different causes for the development of these cracks, which must be looked upon to be an important feature of the structure of concrete with respect to behaviour under load and with respect to failure.

Considering the total lifetime of a concrete member, the earliest cracks are formed by incomplete compaction. Insufficient compaction can lead to local zones of high porosity which act under load like precracked areas. In Table II different stages of strength development and the corresponding crack formation are compiled.

TABLE II
Characteristic periods in the lifetime of concrete and corresponding crack formation.

Stage within Strength Development	Typical Discontinuity
Pouring and Compaction	Compaction Pores
Fresh Concrete	Bleeding Cavities
Hardening Concrete	Thermal Cracks, Chemical and Capillary Shrinkage Cracks
Drying Concrete	Hygral Shrinkage Cracks
Loaded Concrete	Interfacial Cracks, Crack Growth

Immediately after pouring and before hardening, sedimentation (bleeding) takes place. This process causes water filled pockets under coarse aggregates. As a consequence horizontal cracks are formed. This effect obviously causes a certain degree of anisotropy.

As the hydration continues heat of hydration is liberated. Under normal conditions this causes a time-dependent temperature gradient. It can be shown that in many concrete elements thermal cracking takes place in the outer cooler zones. The orientation of these cracks depends on the geometry. There are measures, however, to prevent excessive thermal cracking.

After demoulding, the surface of concrete begins to dry and reaches equilibrium with the environmental humidity very quickly, whereas the centre of a given specimen may remain saturated for many years. This hygral gradient induces shrinkage cracks. Again the orientation of these cracks depends on geometry.

In hardened concrete the interfaces between hardened cement paste and coarse aggregates remain weak for a long time. Therefore comparatively moderate loads, far below the design load, may cause interfacial cracking.

In summary we can conclude that in a concrete specimen some of the causes mentioned in this section and compiled in Table II or combinations of these different causes will introduce cracks into the structure under normal conditions. Some of these cracks are oriented at random and others initiate a certain degree of anisotropy. The observed strength therefore does not only depend on concrete composition but to a large degree on curing conditions.

3.4. Inclusions

According to the Griffith criterion a crack spreads catastrophically once the load becomes critical. There is no stable crack growth and no crack arresting. In a composite material therefore the unmodified Griffith equation is not a realistic approximation for a composite material.

Consider for a moment the situation in normal concrete, where the aggregates are stronger than the matrix. If a crack starts to spread under a given load from a big pore in the weaker matrix or from an interface there is a chance that it will meet an inclusion and then will be stopped. This simplified approach is schematically shown in Figure 9. $2C_M$ is supposed to be the length of the initial crack in the matrix. As soon as σ_M is reached the crack will spead in an unstable way according to :

$$\sigma_M = \frac{2 E \gamma_M}{\pi C_M} \qquad (12)$$

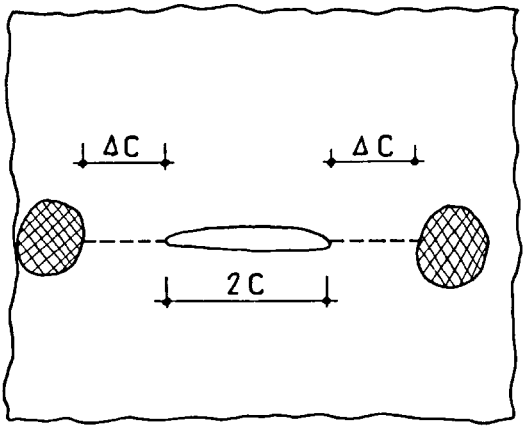

Fig. 9. Schematic representation of a Griffith crack. Once the crack spreads it meets two inclusions after a crack length increase of ΔC.

γ_M denotes the fracture surface energy of the matrix. In this simplified approach we consider in fact a few isolated particles in an otherwise homogeneous matrix, i.e. a diluted system.

Now we suppose that the crack meets an inclusion when it has grown by ΔC. At the crack tip the condition for further crack growth has now changed :

$$\sigma_A = \frac{2\,E\,\gamma_A}{\pi(C_M+\Delta C)} \qquad (13)$$

In this equation γ_A stands for the fracture surface energy of the aggregate. In normal concrete this value is higher than the one of the matrix ($\gamma_A > \gamma_M$) and therefore the resulting curve is shifted towards the right as shown in Figure 10. In the example chosen, the crack runs from point P_1 and is arrested at point P_2. Further crack growth is only possible if the load is increased to σ_A. In point P_3 the condition of crack propagation through the inclusion is fulfilled.

If, however, the crack has increased at least by ΔC' before it meets an inclusion, the crack will not be arrested by the aggregate. This means that crack arresting is not only dependent on the mechanical properties of matrix and aggregates but also on the geometrical distribution. If a crack has already reached a critical length before it meets the aggregate crack, arresting has become impossible. This also explains that beyond a certain critical crack length this

crack arresting mechanism does not work any more and the composite material fails finally in an unstable way.

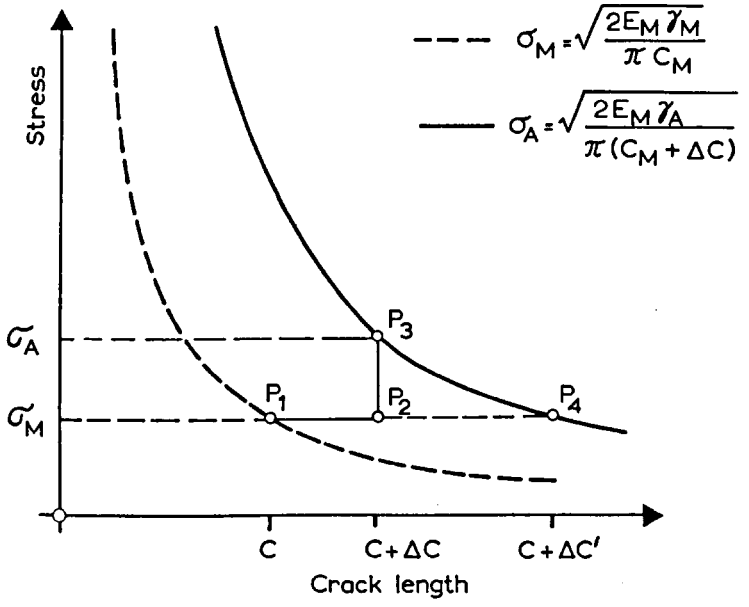

Fig. 10. Schematic representation of equations (12) and (13). If the crack in the matrix becomes critical it will spread from P_1 to P_2. At a higher load σ_A the crack can penetrate the inclusion. If ΔC is large enough so that point P_4 is reached there will be no crack arresting.

3.5 Structural models of Grudemo

In section 3.4 we have discussed the role of hard and strong aggregates as crack arresting inclusions. A sharp crack can also be arrested if it runs into a wide rounded pore. Grudemo has summarized his observations with the electron microscope in the form of simplifying structural sketches (ref. 60 and 61). In this way he designed a possible element of the composite structure of hardened cement paste in which a crack runs into the weak zone around an anhydrous cement particle embedded in hydration products (ref. 61). The sharp crack tip has become rounded and thus the crack is arrested. This situation is schematically shown in Figure 11a.

With the help of another structural model Grudemo points out that a crack will pass different zones such as the lamellar CH phase, inner and outer gel and remaining anhydrous nuclei while it spreads. This simplifying model is shown in

Figure 11b and underlines again the fact that hardened cement paste has to be looked upon to be a heterogeneous composite material. This means that in principle there is no difference between crack formation in hardened cement paste, mortar, and concrete. It is a difference in scale only.

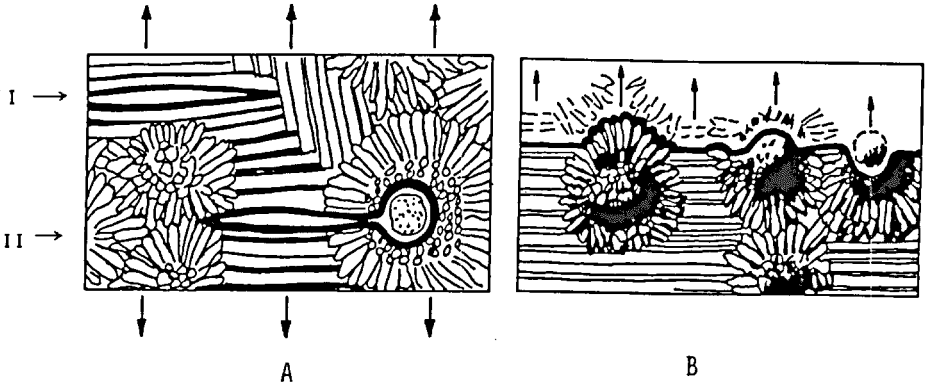

Fig. 11. Idealized details of the gel structure according to Grudemo (ref. 61) :
a) Cracks are arrested either as they meet stronger zones (I) or as they run into rounded-off spaces.
b) The crack runs along cleavage surfaces in lamelar CH phase, zones of contact between gel aggregates, outer and inner gel, and remaining anhydrous nuclei.

3.6 Micromechanics and simulation of composite structures

So far we have given a qualitative description of crack propagation and crack arresting in a composite material. The micromechanics of concrete deal with this subject in more detail and in a quantitative way. In fact a crack, if it is arrested, can propagate through the inclusion or along the interface around it (ref. 62 and 63). The micromechanics of concrete is treated in the theoretical chapter by Zaitsev. Therefore it is not necessary to repeat it here in detail.

We shall, however, mention at this point the possibility of generating composite random structures to simulate the real concrete structure. These computer generated random structures form a basis for the application of micromechanics. In this way many aspects of failure of concrete can be studied systematically. In Figure 12 a computer simulated structure of a matrix with polygonial inclusions is shown. More details are given in chapter 4.2. For this type of a composite material, crack growth can be calculated analytically by means of micromechanics. In addition, typical results are shown as different stages of stable crack growth in Figure 12.

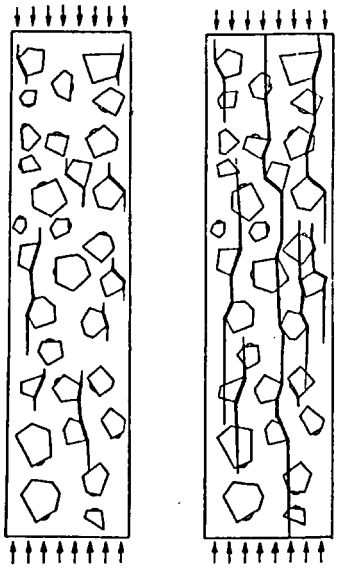

Fig. 12. Simulated composite structure and calculated crack pattern for two different load levels, according to reference (60).

Similar structures can be generated by taking into consideration the random geometry and the size distribution of aggregates (ref. 62). A typical example is shown in Figure 13. In this case, however, crack propagation and crack arresting cannot be treated analytically any more. By means of numerical methods such as finite element analysis it is possible, however, to obtain close approximations of the real fracture process in composite structures.

As a last example for computer generated composite structures, Figure 14 shows a model of concrete with spherical aggregates of different size where the size distribution of the aggregates follows the Fuller function. It is possible to generate in this way three-dimensional structures with spherical aggregates. These three-dimensional composite structures allow us to study crack formation under uniaxial and under multiaxial states of stress.

4. MACRO-LEVEL

On the macro-level the actual macroscopically observed behaviour of a given material has to be described. For numerous materials this can be done by introducing appropriate fracture mechanics parameters. If possible these fracture mechanics parameters have to be linked with structural aspects such as porosity,

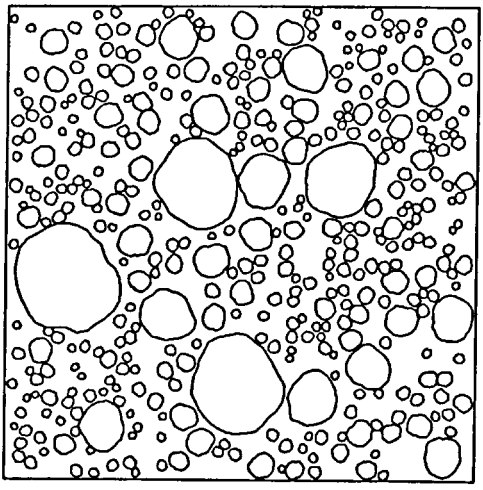

Fig. 13. Simulated structure of concrete with aggregates having random geometry (ref. 62).

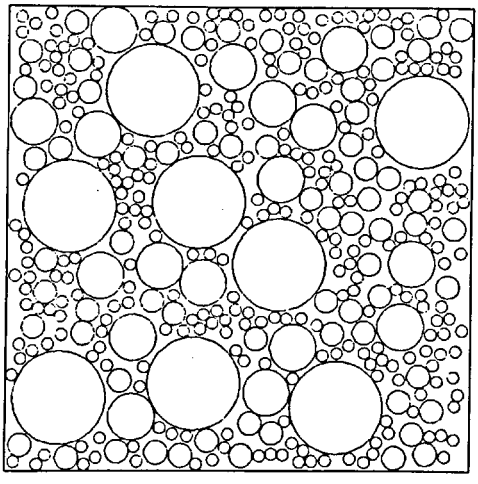

Fig. 14. Simulated structure of concrete with aggregate size distribution following the Fuller curve (ref. 62).

cement content, aggregate size, and aggregate geometry.

In Table III some values for K_{IC} as determined on hardened cement paste, different aggregates and the range observed with concrete specimens are given. Further details on the experimental techniques as well as the results obtained

are described in the corresponding chapters of this volume.

TABLE III
Critical fracture toughness as determined for different hardened cement pastes, aggregates and concrete.

Material		K_{IC} ($MN/m^{3/2}$)	Ref.
Hardened Cement Paste	W/C = 0.30	0.40	
	W/C = 0.36	0.35	66
	W/C = 0.50	0.29	
Aggregates	Limestone	0.70 - 1.00	67
	Marble	1.9	
	Quartz	3.4	68
Concrete		0.70 - 1.50	69

There is an obvious influence of water/cement ratio on K_{IC} (see also ref. 63). This is related to porosity and pore size distribution. K_{IC} for different types of aggregates varies within a wide range. The influence of the age of concrete and of mix proportions on K_{IC} has been studied by various authors (ref. 68). Pak and Trapeznikov have determined experimentally the influence of maximum aggregate size on K_{IC} (ref. 69).

At first glance it seems as if strength and failure process can be adequately described by simple fracture mechanics parameters such as K_{IC} and G_{IC}. Unfortunately this is not the case and these values must be considered to be rough approximations in the case of concrete in particular.

In an attempt to overcome these difficulties, more complex fracture mechanics parameters such as crack opening displacement (COD) and J-integral (see f.e. ref. 70) have been introduced. So far, however, it is not yet possible to discuss the values in relation with the structure of the material.

In addition, fracture mechanics parameters of concrete are not independent of the crack history. As a crack extends a damaged zone the so-called fracture process zone is created ahead of the crack. As a consequence, fracture mechanics parameters increase with crack length until the damaged zone has fully developed. This situation is described by means of the R-curve approach (ref. 71 and 72). It is obvious that the development of the fracture process zone will be stress and time dependent. At present it is unknown in which way the fracture zone depends on the structure of concrete. Further details are described in the contri-

bution of Shah to this volume.

Hillerborg and co-workers developed another approach to describe the failure process of concrete, i.e. the fictitious crack model (ref. 73-75). There is a special section in this volume on this approach. We mentioned already in context with the J-integral and the R-curve that at this moment we cannot discuss these fracture mechanics parameters in terms of structural details mainly because of a lack of suitable experimental data. The same is true for the fictitious crack model. Extensive studies will be necessary to provide a solid basis for a realistic link between the structure of the composite material and fracture mechanics parameters.

On the macro-level appropriate material laws should be formulated. At present it is not yet possible to predict crack resistance if the composition of concrete is known.

5. CONCLUSIONS

The heterogeneous structure of the composite material concrete can be described on three different levels. The physical basis of the xerogel, the binding agent in concrete, is described on the micro-level (Munich Model). This model has proven to be applicable to other cement based xerogels such as aerated concrete (ref. 76). Additional structural details such as pores, cracks and inclusions are introduced on the meso-level. Finally, the macroscopically observed behaviour of concrete is represented on the macro-level.

The influence of porosity, cracks, and inclusions on strength and failure of a composite material can be described in a quasi-quantitative way. K_{IC} and G_{IC} must be looked upon to be rough approximations in the case of concrete. There are different attempts to come to a more realistic description of the failure process such as COD, J-integral, R-curve, and fictitious crack model (FCM). So far, however, existing experimental data do not allow us a rigorous comparison between these more complex fracture mechanics parameters and structural details.

REFERENCES

1 F.H. Wittmann, Modelling of concrete behaviour, Proc. European Concrete Research, Swedish Cement and Concrete Research Institute, Stockholm, 1981, pp. 171-189.

2 F.H. Wittmann, Grundlagen eines Modells zur Beschreibung charakteristischer Eigenschaften des Betons, Deutscher Ausschuss für Stahlbeton, Report Nr. 292, Wilhelm Ernst & Sohn, Berlin (1976).

3 J.F. Young, The microstructure of hardened Portland cement paste, to be published in Z.P. Bazant and F.H. Wittmamm (Ed.) : Creep and Shrinkage in Concrete Structures, Wiley 1982

4 Chemistry of Cement, Proceedings of the 4th International Symposium Washington (1960) edited in 1962.
5 Chemistry of Cement, Proceedings of the 5th International Symposium Tokyo (1968) edited in 1969.
6 Chemistry of Cement, Proceedings of the 6th International Symposium Moscow (Sept. 1974).
7 Chemistry of Cement, Proceedings of the 7th International Symposium Paris (August 1980).
8 T.C. Powers and T.L. Brownyard, Studies of the physical properties of hardened Portland cement paste, Research Laboratories of the Portland Cement Association, Bulletin 22 (1948).
9 A. Grudemo, The microstructures of cement gel phases, Trans. Royal Inst. Techn., Stockholm, Nr.242 (1965).
10 A. Grudemo, An electronmicroscopic study of the morphology and crystallization properties of calcium silicate hydrates, Proceedings Swedish Cement and Concrete Institute Stockholm, Nr. 26 (1955).
11. F. Liebau, Ein Beitrag zur Kristallchemie der Schichtsilikate, Acta Cryst. 824 (1968) pp. 690-699.
12 L.E. Copeland, E. Bodor, T.N. Chang and C.H. Weise, Reactions of tobermorite gel with aluminates, ferrites and sulfates, Res. and Development Laboratories of the Portland Cement Association, Bulletin 211 (1967).
13 W. Richartz and F.M. Locher, Ein Beitrag zur Morphologie und Wasserbindung von Calciumsilikathydraten und zum Gefüge des Zementsteins, Zement-Kalk-Gips, 18 (1965) pp. 449-459.
14 D.L. Kantro, S. Brunauer and C.H. Weise, Development of surface in the hydration of calcium silicates - II. Extension of investigations to earlier and later stages of hydration, J. Phys. Chem., 65 (1962) p. 1804.
15 R.Sh. Mikhail and S.H. Abo-El-Enein, Studies of water and nitrogen adsorption on hardened cement pastes - I. Development of surface in low porosity pastes, Cem. Concr. Res., 2 (1972) pp. 401-414.
16 S. Diamond, Identification of hydrated cement constituents using a scanning electron microscope - Energy dispersive X-ray spectrometer combination, Cem. Concr. Res., 2 (1972) pp. 617-632.
17 U. Ludwig, Investigations on the hydration mechanism of clinker minerals (see ref. 6).
18 H.F.W. Taylor, Crystal chemistry of Portland cement hydration products (see ref. 6).
19 T.C. Powers, Physical properties of cement paste, Research and Development Laboratories of the Portland Cement Association, Res. Dept., Bull. 154 (1960).
20 A. Grudemo, On the development of hydrate crystal morphology in silicate cement binders, Liaisons de Contact dans les Matériaux Composites Utilisés en Génie Civil, RILEM-INSA-Coll., Toulouse, France (November 22-24, 1972).
21 F. Wittmann and G. Englert, Bestimmung der Mikroporenverteilung im Zementstein, Mat. Sci. Eng., 2 (1967) p. 14.
22 M.J. Setzer and F.H. Wittmann, Modified method to calculate pore size distribution using sorption data, Proceedings RILEM-IUPAC International Symposium, Pore Structure and Properties of Materials, Prague (September 18-21, 1973).
23 F.D. Tamas and T.G. Varadi, Role of poly-reactions in the hydration of cement (see ref. 6).
24 L.S. Dent-Glasser, E.E. Lachowski, K. Mohan and H.F.W. Taylor, A multi-method study of C_3S hydration, Cem. Concr. Res., 8 (1978) p. 733.
25 A. Rio and A. Saini, L'industria Italiana del cemento, 39 (1969) p. 867.
26 D.N. Winslow, The specific surface of hardened Portland cement paste as measured by low angle X-ray scattering, Thesis, Purdue University, La Fayette, Indiana, USA (1973).

27 L.E. Copeland and G.J. Verbeck, Structure and properties of hardened cement pastes (see ref. 6).
28 H.F.W. Taylor and D.M. Roy, Structure and composition of hydrates (see ref. 7).
29 P.J. Sereda, R.F. Feldman and V.S. Ramachandran, Structure formation and development in hardened cement pastes (see ref. 7).
30 F.H. Wittmann, Properties of hardened cement paste (see ref. 7).
31 O. Ishai, The time-dependent deformational behaviour of cement paste, mortar and concrete,. Proceedings International Conference, The Structure of Concrete and its Behaviour under Load, London (September, 1965) p. 345.
32 T.C. Powers, Mechanism of shrinkage and reversible creep of hardened cement paste, Proceedings International Conference, The Structure of Concrete and its Behaviour under Load, London (September 1965) p. 319.
33 T.C. Powers, The thermodynamics of volume change and creep, Materials and Structure, 1 (1968) pp. 487-507.
34 J.D. Bernal, Proceedings 3th International Symposium on the Chemistry of Cement, London (1952) p. 216.
35 R.F. Feldman and P.J. Sereda, A model for hydrated Portland cement paste as deduced from sorption - Length change and mechanical properties, Materials and Structures, 1 (1968) pp. 509-520.
36 R.F. Feldman and P.J. Sereda, A new model for hydrated Portland cement and its pratical implications, Engineering Journal, 53 (1970) p. 53.
37 R.F. Feldman, Sorption and length change scanning isotherms of methanol and water on hydrated Portland cement, Proceedings 5th International Symposium on the Chemistry of Cement, Tokyo, Vol. III (1968) p. 53.
38 B.B. Hope and N.H. Brown, A model for the creep of concrete, Cem. Concr. Res., 5 (1975) pp. 577-586.
39 R. Kondo and M. Daimon, Phase composition of hardened cement paste (see ref. 6).
40 F. Wittmann, H. Splittgerber and K. Ebert, Z. Physik, 245 (1971) p. 354.
41 H. Splittgerber and F. Wittmann, Einfluss adsorbierter Wasserfilme auf die van der Waals Kraft zwischen Quarzglasoberflächen, Surface Science, 41 (1974) p. 504.
42 H. Krupp, Particles adhesion, theory and experiments, Advan. Colloid Interfaces Sci., 1 (1967) p. 116.
43 M.J. Setzer and F.H. Wittmann, Surface energy and mechanical behaviour of hardened cement paste. Appl. Physics, 3 (1974) pp. 403-409.
44 H. Ubelhack and F.H. Wittmann, Debye-Waller-facktor of colloidal particles in hydro- and xerogels, Proceedings International Conference on Mössbauer Spectroscopy, Cracow, Vol. 1 (1975) pp. 349-350.
45 B.V. Derjaguin, J. Colloid Interfaces Sci., 49 (1974) p. 249.
46 H. Splittgerber, Spaltdruck zwischen Festkörpern und Auswirkungen an Probleme in der Technik, Cem. Concr. Res., 6 (1976) pp. 29-36.
47 N. Stockhausen, Van der Waals interaction and disjoining pressure between solid surfaces, Proceedings Conference, Hydraulic Cement Pastes; their Structure and Properties, Sheffield (April, 1976) pp. 219-226.
48 F. Schlude and F.H. Wittmann, Uber ein Verfahren zur raschen Bestimmung der komplexen DK im Mikrowellenbereich, Nachrichtentechn. Zeitung, 27 (1974) pp. 365-368.
49 B. Zech and F.H. Wittmann, Studium des dielektrischen Verlhaltens von dünnen adsorbierten Wasserfilmen, Z. Phys. Chemie, NF 92 (1974) pp. 45-62.
50 E.A. Flood, Adsorption potentials, adsorbent self-potentials and thermodynamic equilibria, solid surfaces and the gas-solid interface, Advances in Chemistry Series, Nr. 33 (1961) p. 249.
51 K.G. Krasilnikov, A.M. Podvalny and A.E. Segalov, Self-induced deformations in porous bodies, Kolloidnyi Zhurnal, 36 (1974) pp. 266-271.
52 J.W. Gibbs, Collected works, Yale University Press, New Haven (1957).

53 D.H. Bangham and N. Fakhoury, The swelling of charcoal, Part I : Preliminary experiments with water vapour, carbon dioxide, amonia and sulphur dioxide, Proceedings Royal Society, A130 (1931) pp. 81-89.
54 K.H. Hiller, Strength reduction and length changes in porous glass caused by water vapour adsorption, J. Appl. Phys., 35 (1964) pp. 1622-1628.
55 F.H. Wittmann and J. Zaitsev, Verformung und Bruchvorgang poröser Baustoffe bei kurzzeitiger Belastung und Dauerlast, DAfStb Report, Nr. 232, Wilhelm Ernst & Sohn, Berlin (1972).
56 F. Wittmann, Surface tension, shrinkage and strength of hardened cement paste, Materials and Structures, 1 (1968) pp. 547-552.
57 F.H. Wittmann, The structure of hardened cement paste - A basis for a better understanding of the materials properties, Proceedings Conference, Hydraulic Cement Pastes; their Structure and Properties, Sheffield (April, 1976) pp. 96-117.
58 S.E. Pihlajavaara, A review of some of the main results of a research on the ageing phenomena of concrete : effect of moisture conditions on strength, shrinkage and creep of mature concrete, Cem. Concr. Res., 4 (1974) pp. 761-771.
59 D.D. Higgins and J.E. Bailey, A microstructural investigation of the failure behaviour of cement paste, Proceedings Conference, Hydraulic Cement Pastes; their Structure and Properties, Sheffield (April, 1976) pp. 283-296.
60 A. Grudemo, Strength-structure relationships of cement paste materials, Part 1 and Part 2 CBI Research Reports 6:77 and 8:79, Stockholm (1977 and 1979).
61 A. Grudemo, Microcracks, fracture mechanism, and strength of the cement paste matrix, Cem. Concr. Res., 9 (1979) pp. 19-34.
62 J.B. Zaitsev and F.H. Wittmann, Simulation of crack propagation and failure of concrete, Mat. and Struct., 14 (1981) pp. 357-365.
63 F.H. Wittmann, Mechanisms and mechanics of fracture of concrete, Adv. in Fracture Research, ICF-5, Vol. 4 (1981) pp. 1467-1487.
64 P.E. Roelfstra and H. Sadouki, Simulation des structures composites, Internal Report, Laboratory for Building Materials Science, Swiss Federal Institute of Technology, Lausanne (1981).
65 D.D. Higgins and J.E. Bailey, Fracture measurements on cement paste, J. Mat. Sci., 11 (1976) pp. 1955-2003.
66 R.A. Schmidt, Exp. Mech., 15 (1976) pp. 161-167.
67 B. Hillemeier and H.K. Hilsdorf, Fracture mechanics studies on concrete compounds, Cem. Concr. Res., 7 (1977) pp. 523-536.
68 R.N. Swamy, Fracture mechanics applied to concrete, Chapter 6, in Developments in Concrete Technology, edited by F.D. Lydon, Applied Science Publishers (1979).
69 A.P. Pak and L.P. Trapeznikov, Experimental investigations based on the Griffith-Irwin theory process of the crack development in concrete, Adv. in Fracture Research, ICF-5, Vol. 4 (1981) pp. 1531-1539.
70 S. Mindess, F.V. Lawrence and C.E. Kesler, The J-integral as a fracture criterion for fiber reinforced concrete, Cem. Concr. Res., 7 (1977) pp. 731-742.
71 C. Sok, J. Baron and D. François, Mécanique de la rupture appliquée au béton hydraulique, Cem. Concr. Res., 9 (1979) pp. 641-648.
72 S. Chhuy, M.E. Benkirane, J. Baron and D. François, Crack propagation in prestressed concrete, Interaction with reinforcement, Adv. in Fracture Research, ICF-5, Vol. 4 (1981) pp. 1507-1514.
73 A. Hillerborg, Analysis of fracture by means of the fictitious crack model, particularly for fibre reinforced concrete, Int. J. of Cement Composites, 2 (1980) pp. 177-184.

74 A. Hillerborg and P.E. Petersson, Fracture mechanical calculations, test methods and results for concrete and similar materials, Adv. in Fracture Research, ICF-5, Vol. 4 (1981) pp. 1515-1522.
75 P.E. Petersson, Crack growth and development of fracture zones in plain concrete and similar materials, Lund Institute of Technology, Report TVBM-1006 (1981).
76 Y. Houst, F. Alou and F.H. Wittmann, Influence of moisture content on mechanical properties of autoclaved aerated concrete, in F.H. Wittmann (Ed.) Autoclaved Aerated Concrete, Moisture and Properties, Elsevier, Amsterdam (1983) pp. 219-234.